



## The Implementation of Geopolymers Materials From Moroccan Clay, within the Framework of the Valorization of the Local Natural Resources.

M. Monsif<sup>1,2\*</sup>, S. Rossignol<sup>3</sup>, F. Allali<sup>2</sup>, A. Zerouale<sup>1</sup>, N. Idrissi Kandri<sup>2</sup>, E. Joussein<sup>3</sup>,  
S. Tamburini<sup>4</sup>, R. Bertani<sup>5</sup>

<sup>1</sup> Laboratory of Chemistry of Condensed Matter, Faculty of Sciences and Technology, University of Sidi Mohammed Ben Abdellah, Road Imouzzer- B.P. 2202 Atlas Fez – Morocco

<sup>2</sup> Laboratory of Applied Chemistry, Faculty of Sciences and Technology, University of Sidi Mohammed Ben Abdellah Road Imouzzer- B.P. 2202 Atlas Fez – Morocco

<sup>3</sup> Ceramic European Center, SPCTS UMR 7531, University of Limoges, 12 rue de l'atlantis, France

<sup>4</sup> National Research Council of Italy (CNR), Institute for Energetics and Interphases (IENI), Corso Stati Uniti 4, 35127, Padova, Italy

<sup>5</sup> Department of Industrial Engineering, University of Padova, Via F. Marzolo 9, Padova, Italy

Received: 13 Jan 2017  
Revised: 16 Apr 2017  
Accepted: 18 Apr 2017

### Keywords

- ✓ Moroccan Clay,
- ✓ Characterization,
- ✓ Kaolinite,
- ✓ silicate solution,
- ✓ Geopolymer,
- ✓ Consolidated Materials

[manal.monsif@usmba.ac.ma](mailto:manal.monsif@usmba.ac.ma)  
Phone:  
(+212)615438206

### Abstract

The feasibility of geopolymers from two local Moroccan clays was performed at room temperature, using calcined clay with potassium hydroxide solution as alkaline medium and Potassium silicate solution. Several compositions with different fraction have been prepared up to obtain those with a homogeneous appearance and well consolidated. Used clays have been characterized for their possible use in the synthesis of geopolymer. The combination of the results of different analysis methods; X-ray fluorescence (XRF), X-ray diffraction (XRD), infra-red spectroscopy (FTIR), thermal analysis (DTA-TG), particle size distribution (PSD), specific surface area (BET) and Solid State MASNMR of <sup>29</sup>Si and <sup>27</sup>Al allowed to establish the chemical and mineralogical compositions of the used clays. The chemical analysis showed a dominance of silica SiO<sub>2</sub> and alumina Al<sub>2</sub>O<sub>3</sub>. It demonstrated that the main clay minerals in these samples were kaolinite chlorite and illite with the presence of other minerals. These clays contain two kind of populations; mono-modal and bi-modal with different specific surface area and different behaviors on the thermal analysis depending on their composition. The clay rich kaolinite was thermally treated at 700°C in order to convert it into amorphous metakaolin which is a more reactive precursor for geopolymer synthesis, and then it was characterized by XRD, FTIR and NMR. The calcined clays were tested as potential aluminosilicate sources for the synthesis of geopolymer. The reactions of geopolymerization and the structural evolution of the formed geopolymers were investigated using FTIR spectroscopy.

## 1. Introduction

Clays have an important place in the mineral world, scientific research and environmental sciences. As an abundant and natural material they represent are of interest in ceramic building materials because of their properties such as their thermal conductivity and resistance [1, 2]. The use of clay in a particular industry is mainly related to their physico-chemical and mineralogical compositions, they can be used in many different industrial applications. Kaolinitic clays are significant industrial raw materials used in various manufacturing applications, such as in the construction field, in ceramics processing and in many other sectors for diverse and varied applications [3]. One of the most innovative applications of kaolin is its use as cheaper raw material in the synthesis of geopolymers. Indeed, there has been increasing interest in producing eco-friendly geopolymers from natural, inexpensive clayey materials [4].

Moroccan clays were used for years in the traditional ceramic industry. The recent scientific works aim at valuing these Moroccan ecomaterials in new domains such as nanocomposites [5, 6], mineral membranes and geopolymers [7, 8] which attracted worldwide interests. Many works have been studied on these materials but there is no one with Moroccan clays.

Geopolymers are amorphous three-dimensional aluminosilicate binder materials, which were first introduced by Davidovits [9], these materials are acid-resistant inorganic polymers with zeolitic properties. Geopolymers have been received considerable attention due to their excellent mechanical properties, low shrinkage, fire resistance, low energy consumption [10]. As materials that can be obtained with low carbon emission, the geopolymers offer also solutions to the environmental problems. In the treatment of waste, the geopolymer cements are used for the encapsulation of toxic and radioactive waste [9].

Geopolymerization results from an old principle which is a reaction between amorphous silica and alumina rich solids with a high alkaline solution to form amorphous to semi-crystalline aluminosilicate inorganic polymers [11]. The formation of geopolymers involves a chemical reaction between an aluminosilicate material and sodium silicate solution in a highly alkaline environment. The exact mechanism of geopolymerization is not yet fully understood, but it is believed to consist of three main stages: (1) the dissolution of Al and Si in a highly alkaline solution and diffusion of the dissolved species through the solution, (2) the polycondensation of the Al and Si complexes with the solution and the formation of a gel and (3) the hardening of the gel that results in the final geopolymeric product [12]. This type of materials has the advantage to be able to be formulated from a wide range of minerals of aluminosilicate other than the kaolin and the metakaolin, as the fly ash, the milkmen of blast furnaces or natural minerals as clays.

In this work, the feasibility of geopolymers was estimated at moderate temperature from the Moroccan clays used in traditional activities. The choice of the clay depended on its chemical and mineralogical composition, determined by the physicochemical characterization. Then, the clay was thermally activated, and its structural evolution was verified by XRD, FTIR and NMR and then it was introduced into the geopolymer formulation. The study of the feasibility of these materials with these clays was conducted using FTIR.

## 2. Materials and methods

### 2.1 Materials

Two types of clays were collected from Berrechid and Tiflet (Morocco), denoted as A1 and A4, respectively. The clays were dried at 40°C for two days and then crushed in an impact crusher followed by a planetary crusher in order to be sieved into a fraction inferior to 80 µm and to have a homogeneous particle size ready to be used.

Potassium hydroxide KOH (purity 85.2%) was used with these clays and a metakaolin clay (MT) in an alkaline solution denoted S3 which their composition is reported in table 1.

**Table1:** The chemical composition of the solution S3 and the clay MT.

	S3	MT
% SiO <sub>2</sub>	21.92	55
% K <sub>2</sub> O	18.68	-
% H <sub>2</sub> O	59.40	-
% Al <sub>2</sub> O <sub>3</sub>	-	40

### 2.2 Methods

#### 2.2.1 Characterization

The chemical composition of clays was determined using X-ray fluorescence Spectrometer (XRF) sequential (WD-XRF) Axios of analytical mark with a canal of measure based on a single goniometer covering the complete range of measure going from Boron to uranium.

The distribution of grain size was determined using a Mastersizer 2000 particle size analyzer by laser diffraction type. The powder was suspended by an air current flowing through a glass cell with parallel faces illuminated by a beam of laser light. The measurement is made at a pressure of 3 bars.

The specific surface area (BET) is obtained with Micrometrics Flow Sorb II 2300. The used gas is the nitrogen and the measures are made at 77 K.

The mineralogical phases present in the raw clay were identified by Bruker-AXS D 5005 type Debye-Sherrer using the radiation Cu<sub>Kα</sub> ( $\lambda_{K\alpha} = 1,54056 \text{ \AA}$ ) and a back monochromator in graphite. The range of analysis is

between 2.5 and 65 degree with a step of 0.04 degree and a time of acquisition of 55 min. The present crystalline phases in the material are identified compared with the standards PDF (Powder Diffraction Files) of the ICDD (International Center for Diffraction Dated).

Absorption spectra of the characteristics bands of the samples were determined by Fourier Transform Infrared spectroscopy (FTIR) by ThermoFischer Scientific Nicolet 380 in transmission mode. The KBr pellets with the product or the powder were simply deposited on the diamond before acquisitions. The acquisitions are realized between 400 and 4000  $\text{cm}^{-1}$ , the number of scans is 64 and the resolution is 4  $\text{cm}^{-1}$ . The follow-up of materials studied during their formation is also analyzed by putting a drop of the mixture studied on the diamond substratum. The spectra obtained were corrected by the elimination of the contribution of  $\text{CO}_2$  by establishing a baseline and then standardized in order to be compared.

Solid State MAS NMR experiments were collected on Bruker AVANCE III 300 spectrometer (magnetic field of 7.0 T corresponding to  $^{27}\text{Al}$  and  $^{29}\text{Si}$  Larmor frequencies of 78.066 and 59.623 MHz respectively) equipped for solid-state analysis in 4 mm diameter zirconia rotors with Kel-F caps. The magic angle was accurately adjusted prior to data acquisition using KBr.  $^{29}\text{Si}$  chemical shifts were externally referenced to solid tetrakis(trimethylsilyl)silane at -9.8 ppm (in relation to TMS) and  $^{27}\text{Al}$  chemical shifts were externally referenced to  $\text{AlCl}_3 \cdot 6\text{H}_2\text{O}$  (0 ppm). The semi-quantitative  $^{29}\text{Si}$  single-pulse experiments for A1 and A4 were collected at a spinning frequency of 6 kHz, a recycling delay of 60s and 800 transient for A1 and 4000 for A4.  $^{27}\text{Al}$  experiments were collected at a spinning frequency of 13 kHz with a pulse of 1.0 us and a recycle time of 2 s. About 4000 scans were needed using a single pulse experiment.

Thermogravimetric analyses (DTA-TG) were realized with SDT Q600 under air, between the ambient temperature and at 1400 °C with a heating rate of 5 °C/min under sweeping of air. The samples were held in Pt crucible.

### 2.2.2 Preparation of geopolymer samples

After their characterization, the A1 clay was calcined (A1c) at 700°C for 5 h. The consolidate materials were obtained (Figure 1) by dissolving potassium hydroxide KOH into a commercial potassium silicate solution S3 with Si/K molar ratios of 0.65 and pH values of 14 mixing with A1c, A4 and MT with different fractions. The resulting mixture was placed in a polystyrene mold, which was placed in an oven at 70 °C for 2 h. Then the samples were stored at room temperature (25 °C).

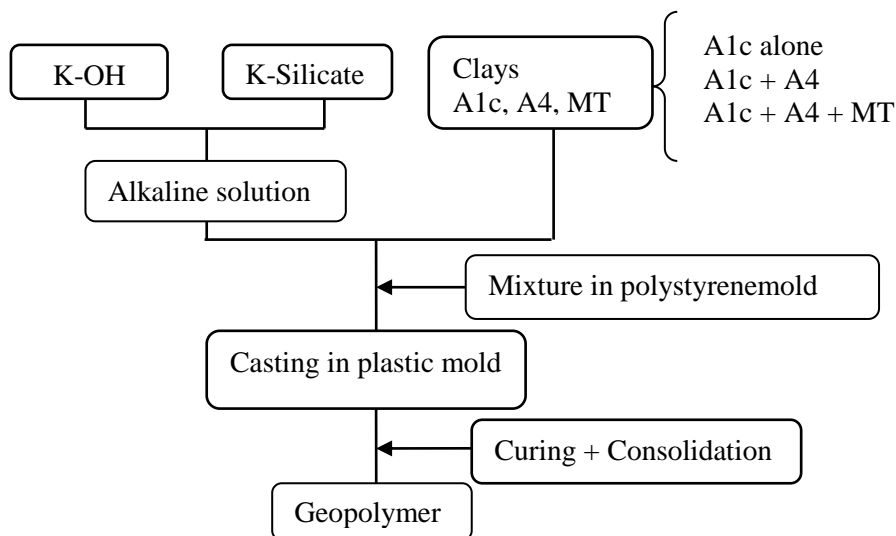


**Figure1:** Schematic process of geopolymer synthesis

## 3. Results and discussion

### 3.1. Clay characterization

#### 3.1.1. Mineralogical composition

The chemical compositions of the studied clay A1 and A4 is presented in Table 2. The most abundant oxides in A1 are silica  $\text{SiO}_2$ , alumina  $\text{Al}_2\text{O}_3$  and iron oxide  $\text{Fe}_2\text{O}_3$  with variable content of 86-88% and predominance of silica (54.5 wt%) indicating that this clay is an ferric aluminosilicate. The A4 clay is rich besides the silica and some alumina with CaO (18.8% wt) it is a calcium aluminosilicate.

The abundance of the kaolinite in the A1 clay is clearly shown by the low amount of MgO (1.76 wt %) and by a mass ratio  $\text{SiO}_2/\text{Al}_2\text{O}_3$  [13, 14] which not exceeds the value of 1.98, contrary to A4 which has 3.29 wt % of MgO and a ratio superior than 2 which indicates the presence of illite [15, 16].

**Table 2:** Chemical composition and weight content of the oxides in the A1 and A4 clays determined by XRF

Samples	Content (weight%)									
	SiO <sub>2</sub>	Al <sub>2</sub> O <sub>3</sub>	Fe <sub>2</sub> O <sub>3</sub>	K <sub>2</sub> O	MgO	Na <sub>2</sub> O	CaO	TiO <sub>2</sub>	P <sub>2</sub> O <sub>5</sub>	L.I.
A1	54.50	27.4	4.89	<b>1.92</b>	1.76	1.24	0.31	0.85	0.23	6.65
A4	42.6	11	2.32	1.3	3.29	0.82	<b>18.8</b>	0.44	0.24	<b>18.7</b>

(L.I.: Loss on ignition at 1000°C)

### 3.1.2. Structure analysis using XRD and FTIR

The mineralogical composition reported by XRD spectra of A1 (figure 2) and A4 (figure 3) shows a predominance of quartz ( $\text{SiO}_2$ ) with the presence of clay minerals having different intensities which are chlorite ( $(\text{Mg,Fe,Al})_6[\text{AlSi}_3\text{O}_{10}](\text{OH})_8$ ), kaolinite ( $\text{Al}_2\text{Si}_2\text{O}_5(\text{OH})_4$ ), muscovite ( $\text{KAl}_2[(\text{Si}_3\text{Al})\text{O}_{10}](\text{OH})_2$ ) and illite ( $(\text{K}_{0.7}\text{Na}_{0.01}\text{Mg}_{0.15}\text{Fe}_{0.04}\text{Al}_{2.59}\text{Si}_{3.27}\text{O}_{10}(\text{OH})_2$ ). The diffraction peaks of illite very close to those of muscovite do not allow differentiating these phases easily without preliminary treatment [17]. Furthermore, diffractograms present also the diffraction belonging to the calcite  $\text{CaCO}_3$ , the dolomite  $\text{MgCa}(\text{CO}_3)_2$  and the hematite  $\text{Fe}_2\text{O}_3$ . In the sample A4 the phases of carbonate are dominant which is in consistent with the previously obtained results of XRF. The XRD pattern of A1 clay is characteristic of kaolinite and chlorite, with small amount of muscovite, calcite and hematite. Theoretically, the presence of chlorite is expected with the iron content in the sample, this was shown by name [18] and it is in accordance with our result which indicates the presence of hematite and chlorite. The A4 clay contains less kaolinite and this result is in agreement with that of the chemical analysis.

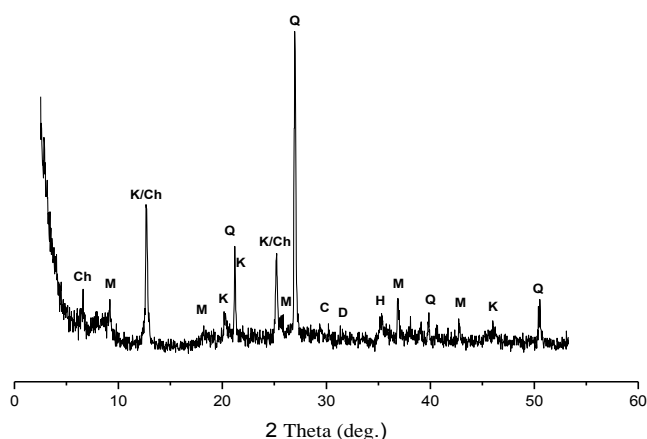


**Figure 2:** Diffractogram on clay powder A1  
Ch: Chlorite, K: Kaolinite, Q: Quartz, I: Illite, D: Dolomite,  
M : Muscovite, C : Calcite, H : Hematite

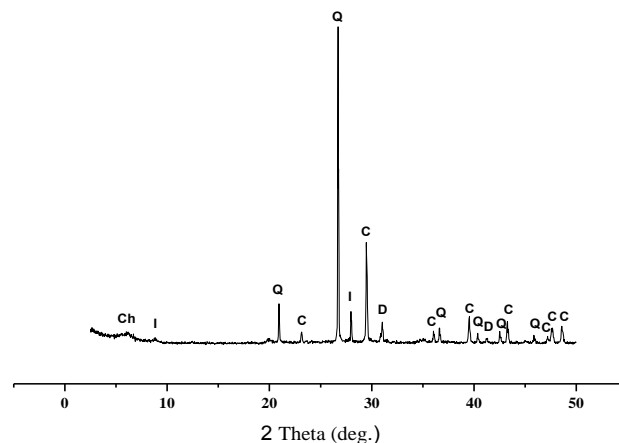


**Figure 3:** Diffractogram on clay powder A4  
Ch: Chlorite, Q: Quartz, I: Illite, D: Dolomite, C : Calcite

The FTIR spectrums of studied A1 clays (Figure 4) and A4 (Figure 5) show the presence of kaolinite bands at 3699, 3622, 935, 781, 536  $\text{cm}^{-1}$  [19], illite bands at 3620  $\text{cm}^{-1}$  coupled to the presence of the doublet at 831  $\text{cm}^{-1}$  and 755  $\text{cm}^{-1}$ .

We observed the appearance of two bands at the interval 3600-3700  $\text{cm}^{-1}$ , corresponding to the stretching vibration of the OH groups of the octahedral group bonded to two Aluminium atoms at 3622  $\text{cm}^{-1}$  and 3699  $\text{cm}^{-1}$  [20]. The intense band situated between 900-1200  $\text{cm}^{-1}$  and centered around 1000  $\text{cm}^{-1}$  is characteristic of the stretching vibrations of the Si-O bond, while the band of deformation of this connection located at 536  $\text{cm}^{-1}$  [21, 22] which confirms the presence of the kaolinite in the clay.

The shoulder located between 3500 and 3236  $\text{cm}^{-1}$  is attributed to the deformation vibrations of H<sub>2</sub>O molecule [23]. Bands which range between 1636-1640  $\text{cm}^{-1}$  are assigned to the stretching vibrations of the OH group of water of constitution and to deformation vibrations of adsorbed water [24].

The calcium carbonate characterized by an infrared band near to 1426  $\text{cm}^{-1}$  and two peaks at 876 and 714  $\text{cm}^{-1}$ . These three bands of absorptions are respectively assigned to the asymmetrical and symmetrical vibration of the C-O bond, and their deformations [25]. The presence of CaCO<sub>3</sub> in these samples is shown by the band at 1426  $\text{cm}^{-1}$  [26-28]. The spectrum of A4 clay presents the most intense bands and well resolved by these bonds, which is in agreement with the results of the chemical analysis and XRD.

The various silicon bonds are characterized by the vibration bands at 1105  $\text{cm}^{-1}$  for Si-O [26], a band of symmetric deformation at 694  $\text{cm}^{-1}$  for Si-O-Si [23], 521  $\text{cm}^{-1}$  for Si-O-Al and 509  $\text{cm}^{-1}$  for Si-O-Fe and the bands at 471  $\text{cm}^{-1}$  for Si-O-Si and 431  $\text{cm}^{-1}$  for Si-O-Mg.

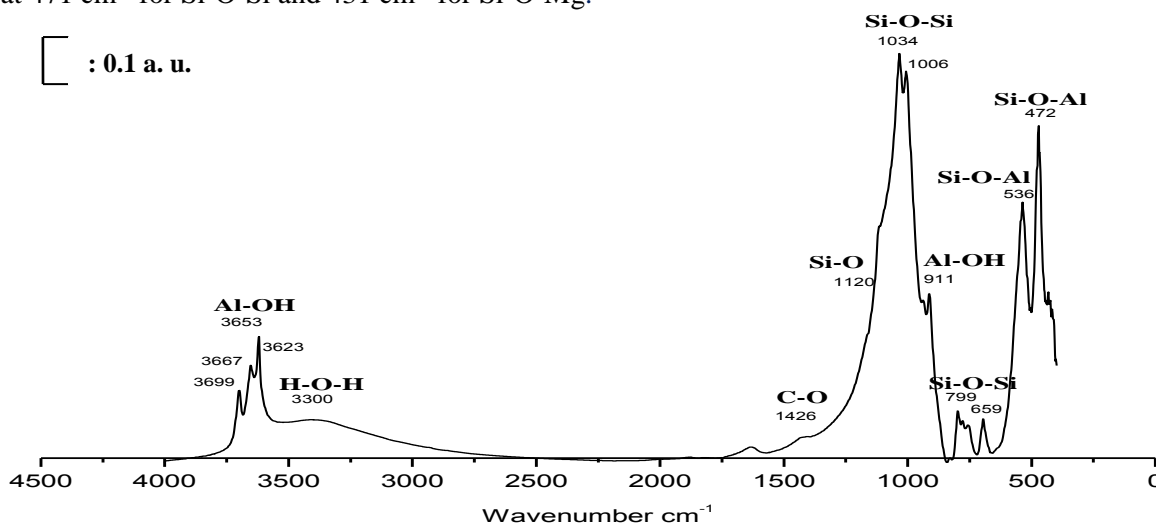


Figure 4: FT-IR spectra of the clay A1

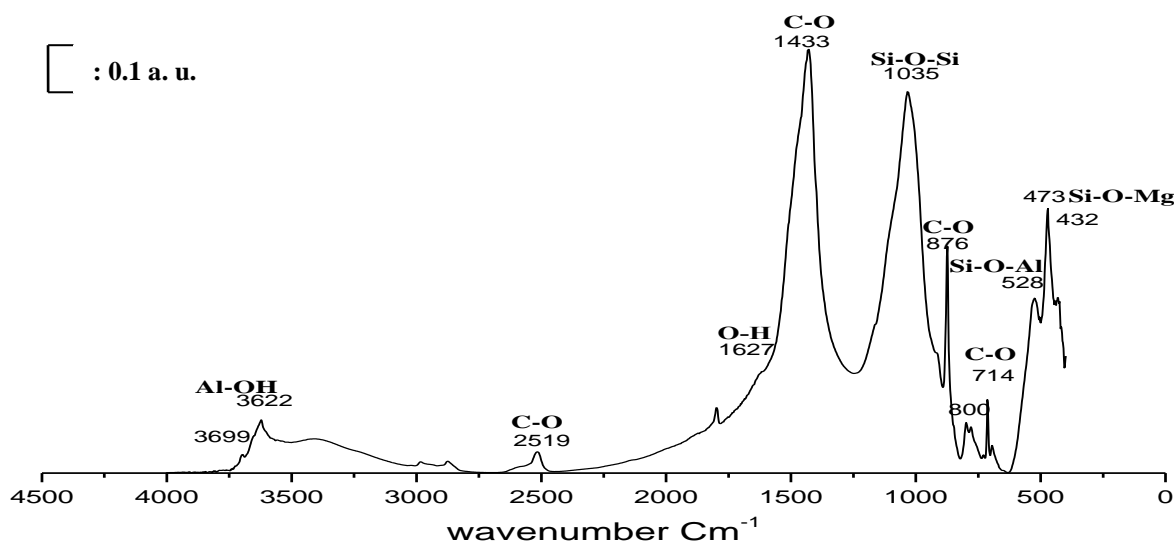
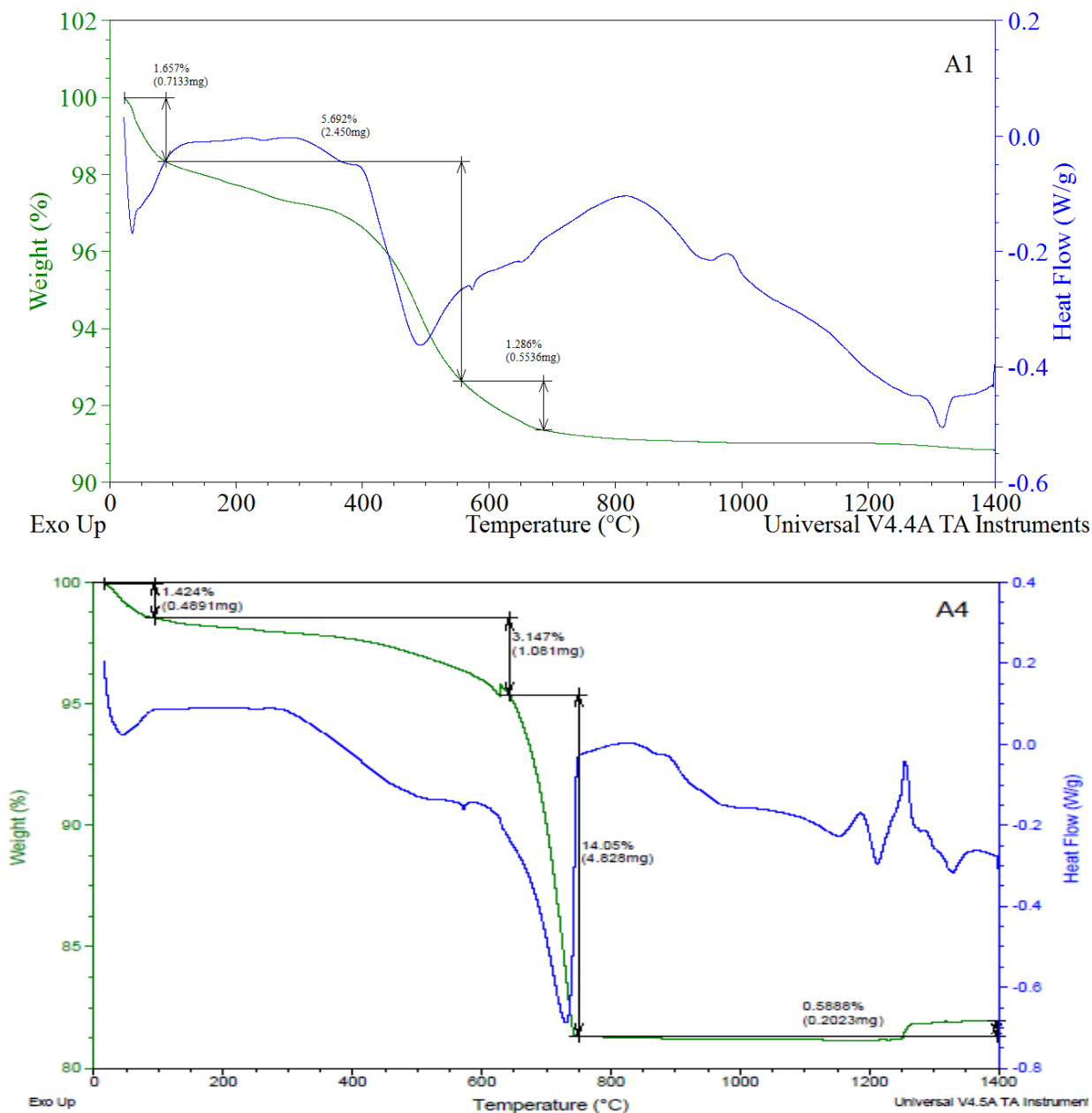


Figure 5: FT-IR spectra of the clay A4

### 3.1.3. Thermal analysis

The thermal analysis curves of A1 and A4 (figure 6) showed the rate of weight loss of these samples versus temperature. The total mass loss of A1 and A4 were respectively 8.97 and 18.71%.

The curve of A1 showed five consecutive endothermic peaks with different losses of mass followed by an exothermic shoulder without loss of mass and one exothermic peak. The first one situated in approximately 100 °C corresponds to the dehydration. The second located between 250 and 300 °C corresponds to the decomposition of ferric compounds such as hematite. The dehydroxylation of kaolinite took place between 480 and 550 °C with a maximum towards 530 °C [29, 30]. The peak observed between 580 and 600 °C corresponds to the conversion of quartz  $\alpha$  to the quartz  $\beta$ . The last endothermic peaks between 630 and 710 °C are associated with the decomposition of carbonates. The shoulder between 700-940 °C is characteristic of the structural reorganization of the metakaolin. The formation of spinel or mullite appears by the exothermic peak between 950 and 1000 °C.



**Figure 6:** Thermal analysis curves of the two clays A1 and A4

The curves of A4 undergo three endothermic dehydration phenomena towards 100 °C, of the deshydroxylation at 560 °C and of the decarbonation in 740 °C, the latter accompanied by the loss of the higher mass compared to the other sample revealing its richness in carbonates (dolomite  $MgCa(CO_3)_2$  and  $CaCO_3$  calcite). Followed by three exothermic peaks, the first two without modifications on the mass and they correspond to a structural

reorganization since this clay does not contain a big proportion of kaolinite, the third accompanied by an increase of mass which is explained by the formation of phases such as mullite and spinel. From the weight losses of different clay materials, the quantification of kaolinite content from the dehydroxylation reactions can be performed. It was found that the kaolinite contents were respectively 40.82 and 22.56 % for A1 and A4.

#### 3.1.4. $^{29}\text{Si}$ MAS NMR of clays

The solid state  $^{29}\text{Si}$  MAS NMR spectrum of the A1 (figure 7) shows a main peak at  $-93.2$  ppm consistent with the Q3 (0Al) environment of  $\text{SiO}_4$  sites in the tetrahedral layer of kaolinite phase [31]. The presence of  $\text{Fe}^{3+}$  (ca.5% w/w) in the A1 causes a fast longitudinal and transversal relaxation so broadening the spectra. The small shoulder at ca.  $-86.5$  ppm to the dominant Q3 peak of the spectrum is indicative of the muscovite/chlorite components. The presence of quartz, underestimated because of long  $^{29}\text{Si}$  longitudinal relaxation time, is confirmed at  $-109.1$  ppm. As evidenced in the XRD spectra, the major constituent of silica of the A4 clay is the quartz phase. As shown in Fig 7 the high relative amounts of the peak related to quartz at  $-107.3$  ppm despite the underestimation due to the long relaxation time, confirm the presence of a moderate amount of amorphous kaolinite at  $-91.5$  ppm as previous quantified by FTIR and TG experiments in addition to other Q3 phase of illite at  $-86.0$  ppm.

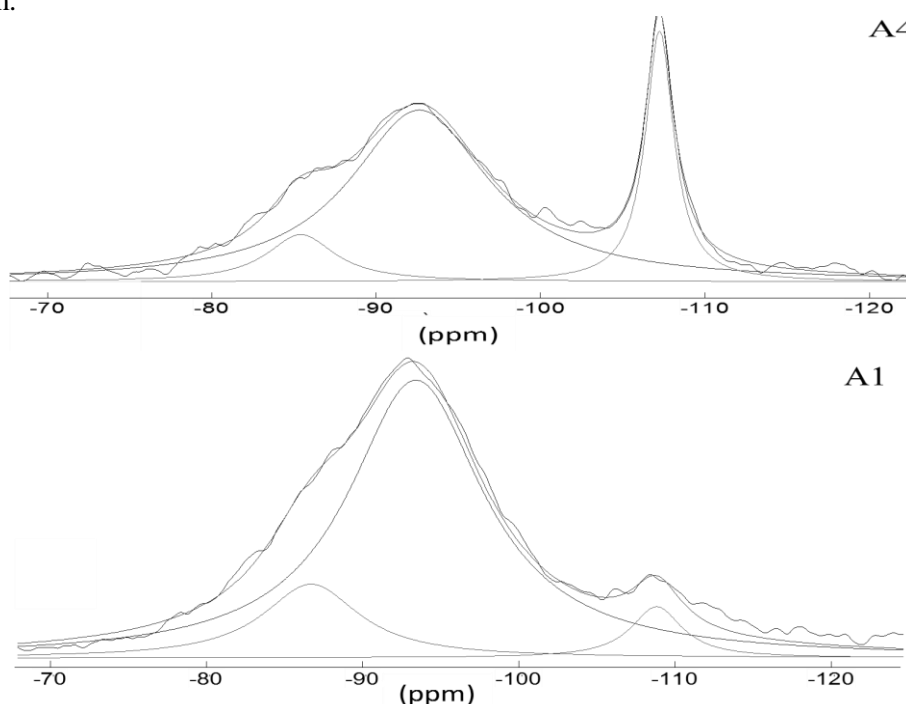


**Figure 7:**  $^{29}\text{Si}$  NMR spectra of A1 and A4 clays

#### 3.1.5. Particle size distribution

Figure 8 reports the particle size distribution of the raw clays, it showed a mono-modal distribution for A1 and bi-modal distribution for A4, this indicates that the reactivity of this clay is lower than that of A1. The comparison between the clays particle size distribution shows that the samples are composed of three populations due to the presence of three main fractions. First one represents the clay fraction ( $<2 \mu\text{m}$ ), many research showed that particle size of clay minerals are generally less than  $2 \mu\text{m}$  [32,33]. The second is between  $2$  and  $20 \mu\text{m}$  corresponding to silt fraction and the last one, the remaining fraction coarser than  $20 \mu\text{m}$  of non-clay minerals, generally quartz. The clay A1 and A4 contain respectively 8% and 4% of clay minerals, whereas clay A4 is rich with larger particles of non-clay minerals. Particle size distribution is one of the most important physical parameters impacting on geopolymer synthesis from aluminosilicates as well as on resulting products since a significant part of the reaction occurs at the particle–liquid interface. Thus, for a given aluminosilicate raw material, the smallest and most porous microstructure particles are most active in an alkaline medium [34,35].

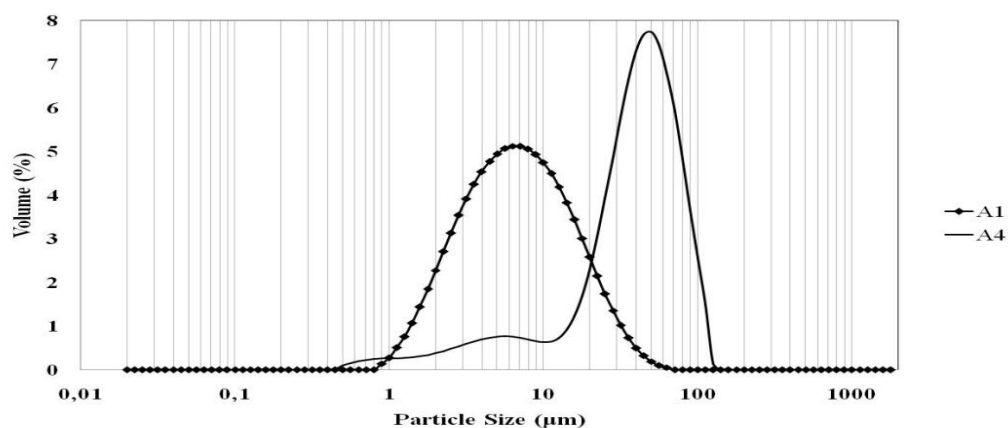


**Figure 8:** Particle size distribution curve by volume of the A1 and A4 clays

### 3.1.6. Specific surface area

The values of the specific surface area for both A1 and A4 clays were nearly of the same order ( $\approx 20 \text{ m}^2 / \text{g}$ ) but it shows a better reactivity for A1 which is rich of clay minerals. This result is in an agreement with the results obtained from the analysis of the particle size distributions. This difference is probably explained by the different mineralogical processing between clays [36].

### 3.2. Effect of the thermal treatment

The clay A1 was chosen for the preparation of geopolymers and the clay A4 was used as additive to verify the influence of calcite and dolomite on the reaction of geopolymerization.

The clays A1 and A4 were calcined at a temperature of  $700 \text{ }^\circ\text{C}$  for 5h and they were characterized by X-ray diffraction (figure 9), infrared spectroscopy (figure 10) and the  $^{29}\text{Si}$  MAS NMR (figure 11). The results of calcined clays were compared to those of untreated clays.

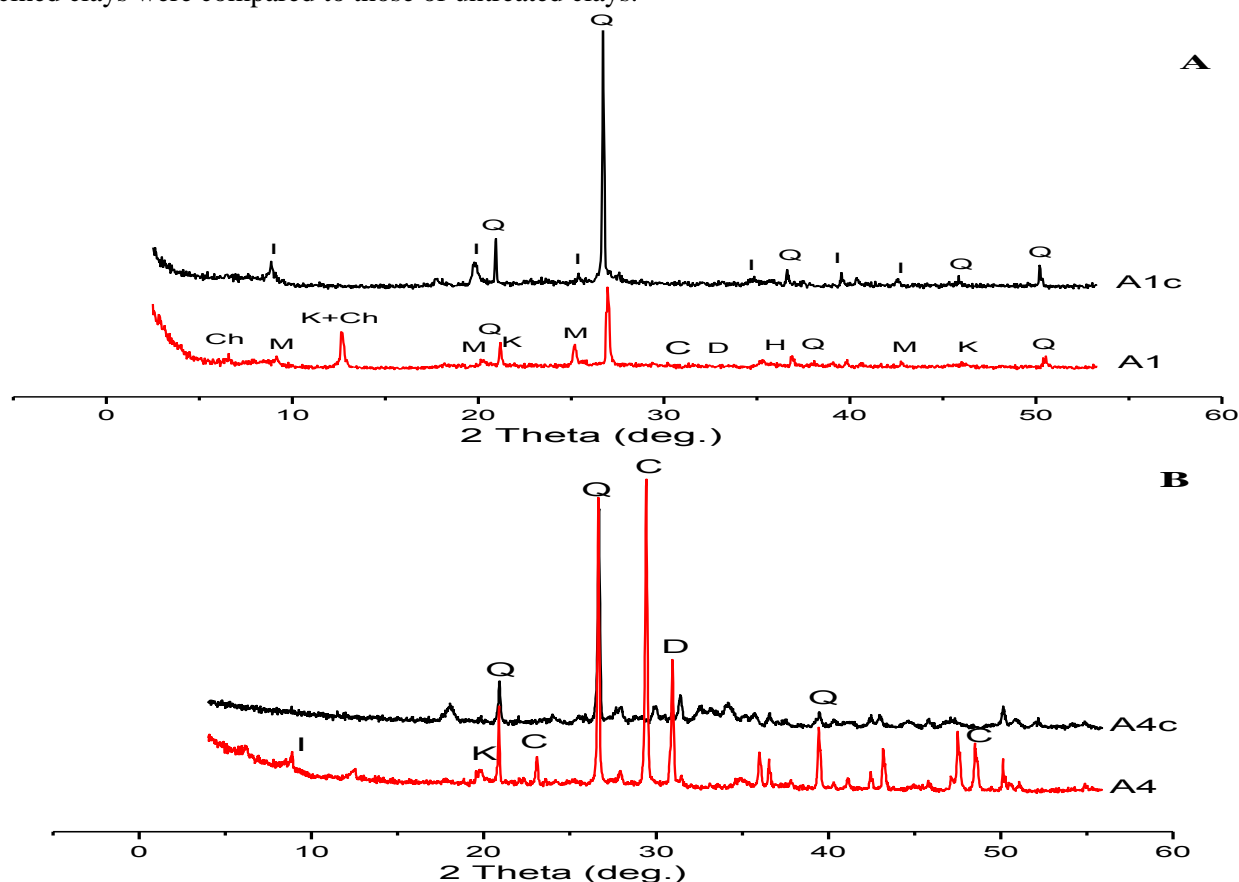


**Figure 9:** Diffractograms of the clay (A) A1 and the clay A1 calcined (A1c), (B) A4 and the A4 calcined (A4c)  
Ch: Chlorite, K: Kaolinite, Q: Quartz, I: Illite, D: Dolomite, M : Muscovite, C : Calcite, H : Hematite

After the thermal treatment, the XRD results showed the disappearance of the peaks of kaolinite, chlorite and carbonates with the persistence of quartz and micas peaks.

The results of FTIR (Figure 10) for A1 confirmed those of its XRD (figure 9), it revealed substantial evidence of change in structure resulting from the thermal treatment and which corresponds to the same changes demonstrated by DTA-TG until this temperature of calcinations (figure 6). It showed the disappearance of stretching bands of kaolinite between 3500 and 3700  $\text{cm}^{-1}$ , the reduction of those of illite also the bands at 3500-3263  $\text{cm}^{-1}$  and 1636  $\text{cm}^{-1}$  corresponds to deformation vibration of H-O-H bonds and elongation of O-H groups of molecules water and Al-OH characteristic of the dehydroxylation of kaolinite ( $\text{Al}_2\text{Si}_2\text{O}_5(\text{OH})_4 + 2\text{H}_2\text{O} \rightarrow \text{Al}_2\text{Si}_2\text{O}_7$ ). There were no changes in characteristic band of quartz.

The transformation of kaolinite into metakaolin was also confirmed by the absence of Al-OH bands at 915 and 939  $\text{cm}^{-1}$ . The amount of the amorphous phase was modified in the clays and increased due to dehydration phenomena in this range of this temperature. It was observed for A4c the decrease of characteristic bands of carbonate between at 1433  $\text{cm}^{-1}$ .

According to XRD diffractogram and FTIR spectra this temperature of calcinations of 700  $^\circ\text{C}$  was sufficient to convert crystalline structure of kaolin to metakaolin (Table 3).

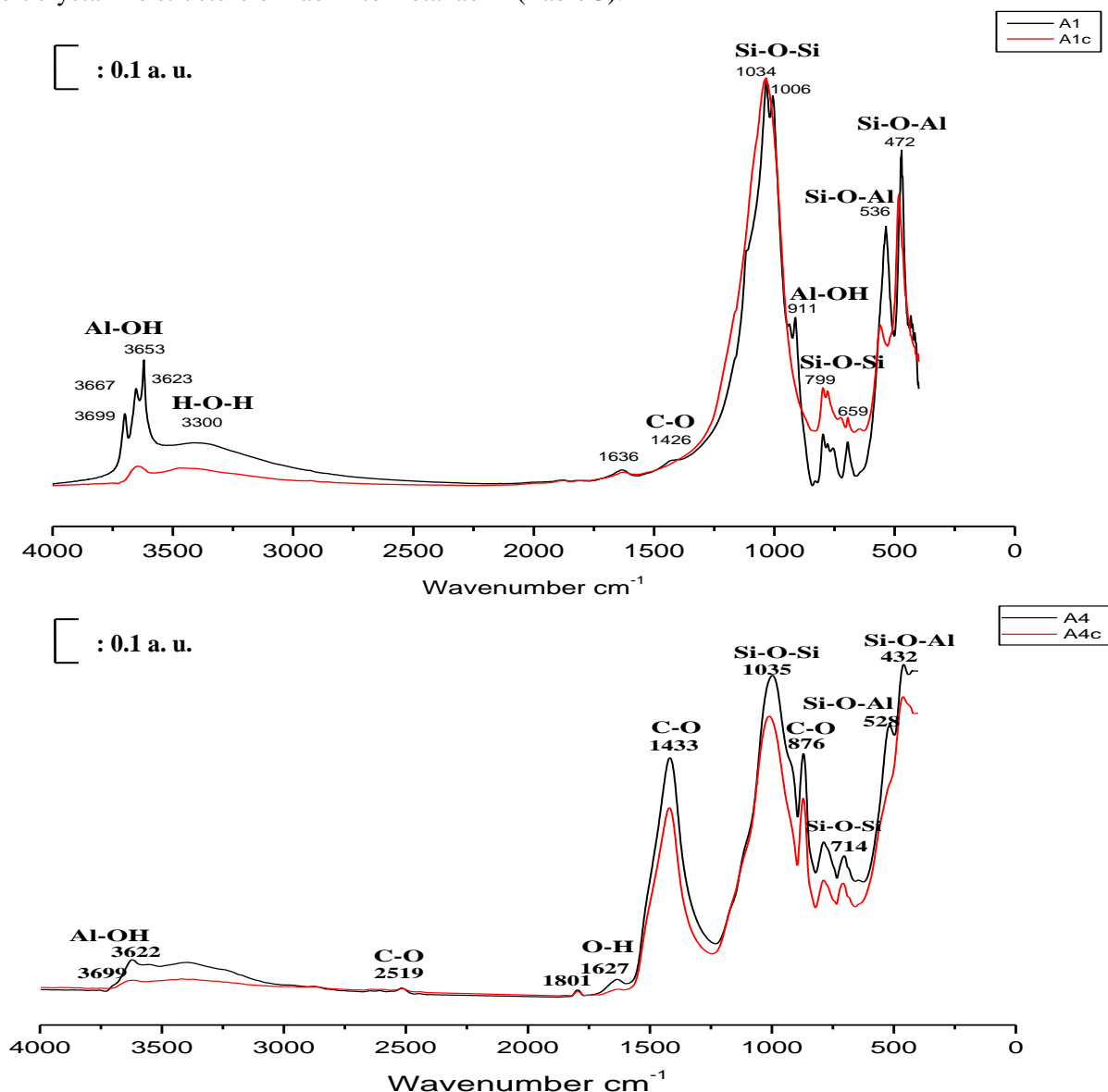


Figure 10: FTIR of the clays A1 and A4 before and after calcination

**Table 3:** Results of characterization of the clay A1 calcined (A1c) in comparison with A1.

		<b>A1</b>	<b>A1c</b>	<b>A4</b>	<b>A4c</b>
<b>XRD</b>		Quartz	Quartz	Quartz	Quartz
		Kaolinite	-----	-----	-----
		Muscovite	Illite	Illite	Illite
		Chlorite	Chlorite	Chlorite	Chlorite
		Calcite	-----	Calcite	-----
		Dolomite	-----	Dolomite	-----
		Hematite	-----	-----	-----
		Anatase	Anatase	-----	-----
<b>FTIR (cm<sup>-1</sup>)</b>					
	<b>Kaolinite</b> $\nu_{\text{Al-OH}}$ [19]	3699–3667- 3653-3623	3649 (small broadband)	1699- 1655- 3622 (low intensity)	3652 (small broadband)
	<b>H-O-H (Water of humidity)</b> [23]	[3500—3263]	-----	[3500—3263]	-----
	<b>OH</b> (Interfoliar water) [24]	1636	-----	1636	-----
	$\nu_{\text{as}}\text{C-O}$ [26-28]	1426	-----	2519 (Dolomite) 1429	-----
	$\nu_{\text{as}}\text{Si-O}$ $\nu_{\text{as}}\text{Si-O-Si}$	1120-1034-1006	1038-1035	1035	1036
	$\delta\text{Al-OH}$	935-911	-----	914	-----
	$\delta\text{Al-O-Si}$	831	-----	-----	-----
	$\nu_{\text{s}}\text{C-O}$	-----	-----	876	-----
	<b>Doublet of quartz</b>	799-781	800-782	799-781	799-781
	$\delta\text{Si-O-Al}^{\text{IV}}$	755	729 (Band moved with low intensity)	-----	-----
	$\delta\text{C-O}$	-----	-----	728 (Dolomite) 714 (Calcite)	728(Low intensity) 714
	$\nu_{\text{s}}\text{Si-O-Si}$ [23]	695	697 (Band moved with low intensity)	695	-----
	$\delta\text{Si-O-Al}^{\text{VI}}$ [21-22]	536	561	528	-----
	<b>Fe-O-Fe</b>	509	-----	-----	-----
	$\delta\text{Si-O-Si}$	472-467	485	-----	-----
	<b>Si-O-Mg</b>	432	-----	431	-----

The  $^{29}\text{Si}$  NMR spectra of A1 and A4 after the thermal treatment at  $700^\circ\text{C}$  (Figure 11) make in evidences the differences of the moroccan clays. Whilst the A1 clay shows the usual evolution of muscovite (dehydration of illite) and kaolinite (dehydration to form metakaolinite) at that temperature (two main broad peaks at -90 and -98 ppm of the dehydroxylated clays plus the unchanged quartz at -107 ppm the A4 clay undergoes a transformation due to the high quantity of Ca carbonates of the starting material. The evolution of the spectra at increasing temperature (not shown) evidence the progressive disappearance of the broad peak assigned to Q3 phases of the clay and the growth of the peak at -72 ppm, indicative of the sorosilicate Q1 gehlenite amorphous phase [37]. This behavior confirms the low geopolymeric activity of the calcinated A4 clay due to absence of metakaolinic phase.

The  $^{27}\text{Al}$  MAS NMR spectra of of A1 and A1c after the thermal treatment at  $700^\circ\text{C}$  (Figure 12) showed two distinct peaks at ca. -4 and 2 ppm normally assigned to six-fold (Al(VI)) coordinated aluminum and at ca. 64 and 61 ppm for the four-(Al(IV)) environments. The A spectrum is the sum of the two components already evidenced in the  $^{29}\text{Si}$  data: the hexa coordinated aluminium in the kaolinitic phase and the presence of Al in the tetrahedral sheet on some illite layers[38]. At high temperature the dehydration of kaolinite is the biggest contribute to the growth of the sharp signal at 61 ppm.

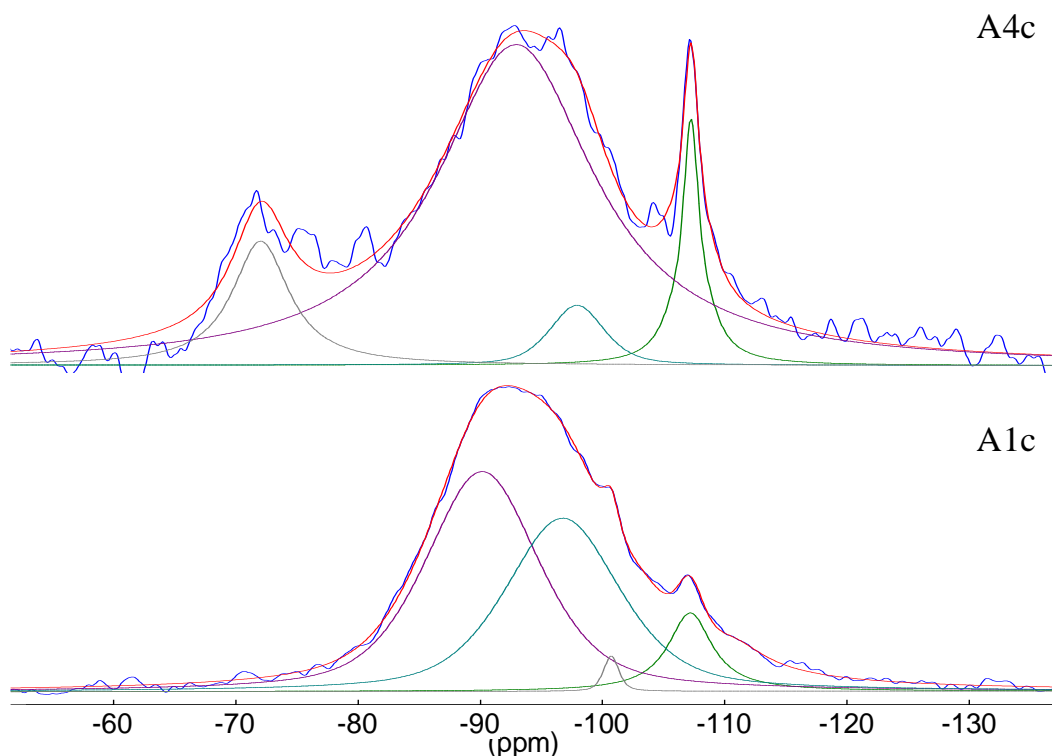


**Figure 11:**  $^{29}\text{Si}$  NMR of A1c and A4c after treatment at  $700^\circ\text{C}$

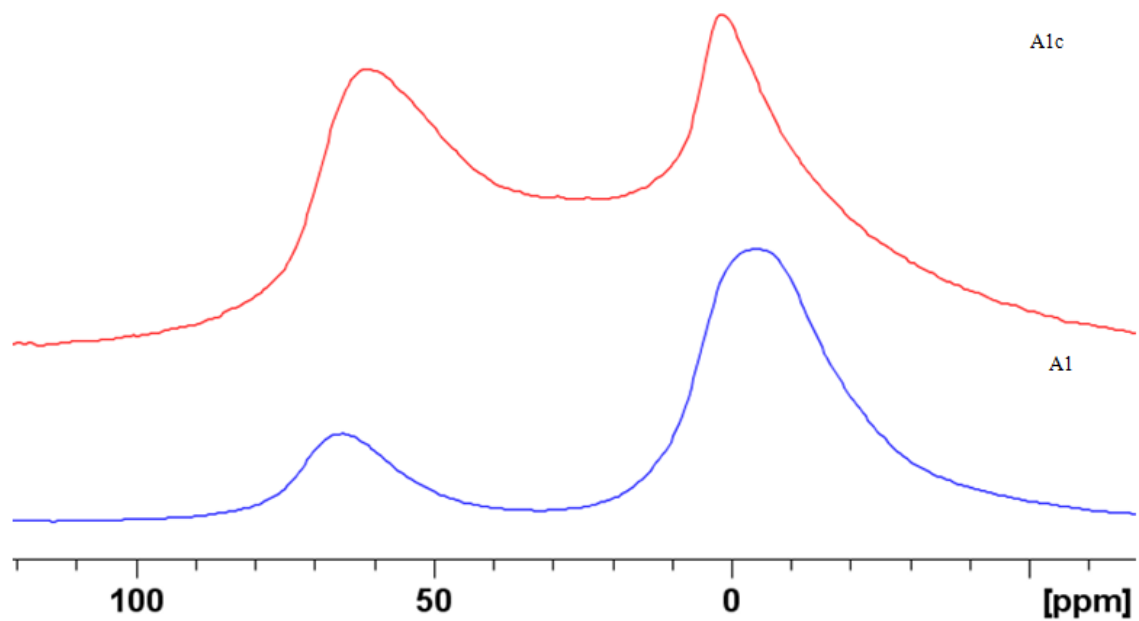


**Figure 12:**  $^{27}\text{Al}$  NMR of A1 at room temperature and A1c at 700°C

### 3.3. Feasibility of consolidated materials

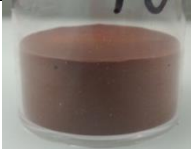
The consolidated materials were obtained by a reaction mixture of the same quantity of KOH, and the alkaline solution S3 with different masses from A1c clay already calcined and A4 or metakaolin (MT) mixed together.

**Table 4:** The chemical composition of the used reactants

	<b>S3</b>	<b>MT</b>	<b>A1c</b>	<b>A4</b>
<b>% SiO<sub>2</sub></b>	21.92	55	59.69	42.6
<b>% K<sub>2</sub>O</b>	18.68	-	1.92	1.3
<b>% H<sub>2</sub>O</b>	59.4	-	-	-
<b>% Al<sub>2</sub>O<sub>3</sub></b>	-	40	27.40	11
<b>% CaO</b>	-	-	0.31	18.8

Table 5 shows the photos of different obtained consolidated materials and the percentage of different elements present on the mixture.

**Table 5:** Composition of the various mixtures

Samples	Used clay	Elements Percentage (%) in the mixture				Photos
		Si	Al	K	Ca	
C2	A1c	54.61	20.82	27.27	0.29	
C3	A1c+A4	50.33	17.07	28.35	4.27	
C5	A1c+A4	52.04	20.15	24.24	3.57	
C6	A1c+A4	53.40	22.54	21.00	3.06	
C14	A1c	53.77	23.42	19.76	3.05	
C15	A1c+A4	52.83	21.46	22.41	3.30	
C19	A1c+A4+MT	52.22	22.25	22.25	3.28	
C20	A1c+A4+MT	52.94	23.31	20.70	3.05	

The synthesized materials show a brown color and different characters; laminated, cracked, pasty and consolidated. The presence of a gel deposit or an heterogeneous materials, indicate the difficulties in obtaining a

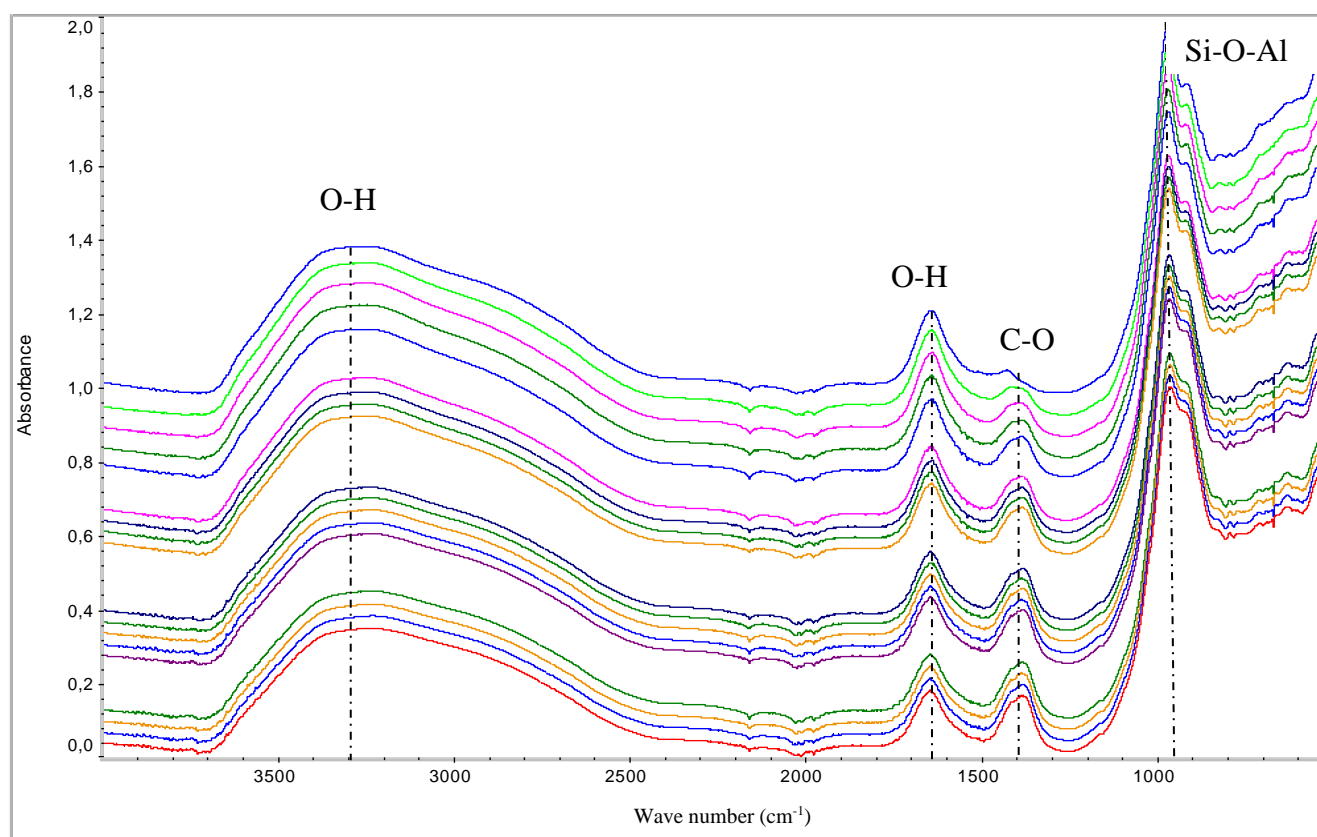
consolidated materials, also suggest that not all of the alkaline solution reacted due to the lack of reactive species in calcined material.

The compositions presented on the table 4 shows the different possibilities to obtain consolidated materials exempt from defects. These materials have been synthesized using A1, A1c, and A4 clays. The first try based on A1 only gave heterogeneous mixtures and pasty with the appearance of two phases. However the compositions obtained from A1c was consolidated (C14 and C20) which justify the activation of this clay by the calcinations.

The first test using both clays A4 with A1c, we obtained an heterogeneous mixture consists of two viscous phases (gel), to improve the composition, it was over by A1c with different masses from 66%, up to obtain the composition C5, C6 and C15. We have also tried in C19 to use pure metakaolin, by reducing the amount of A1c and replace it with MT, it allowed us to obtain a better consolidated material.

According to the literature, geopolymers are synthesized by polycondensation of  $[\text{SiO}_4]$  and  $[\text{AlO}_4]$  tetrahedral in alkali activated aqueous solutions, so the polymerization reaction requires a sufficient amount of silica and aluminum. However our clays contain different amounts which explains the results obtained from A1, a rich clay kaolin which ensure at the same time good reactivity after calcination due to its activation and also a good source of alumina and silica compared with A4 but not sufficient for a reaction of geopolymerization in an alkaline medium to form free  $\text{SiO}_4$  and  $\text{AlO}_4$  tetrahedral units.

The mechanism of geopolymerization is translated by a modification of the structure of the material, which is an evolution of the bonds between atoms. It is possible to follow this restructuring over time by infrared spectroscopy. For that purpose, in order to correlate all of the results on the consolidated materials a drop of mixture was deposited on the diamond, just after the addition of clay. So the study is more made on a punctual acquisition but on all the acquisitions realized in real time every 10 minutes for 13 hours. This allows following the evolution of the bonds within the drop during the consolidation of the material (Figure 13).



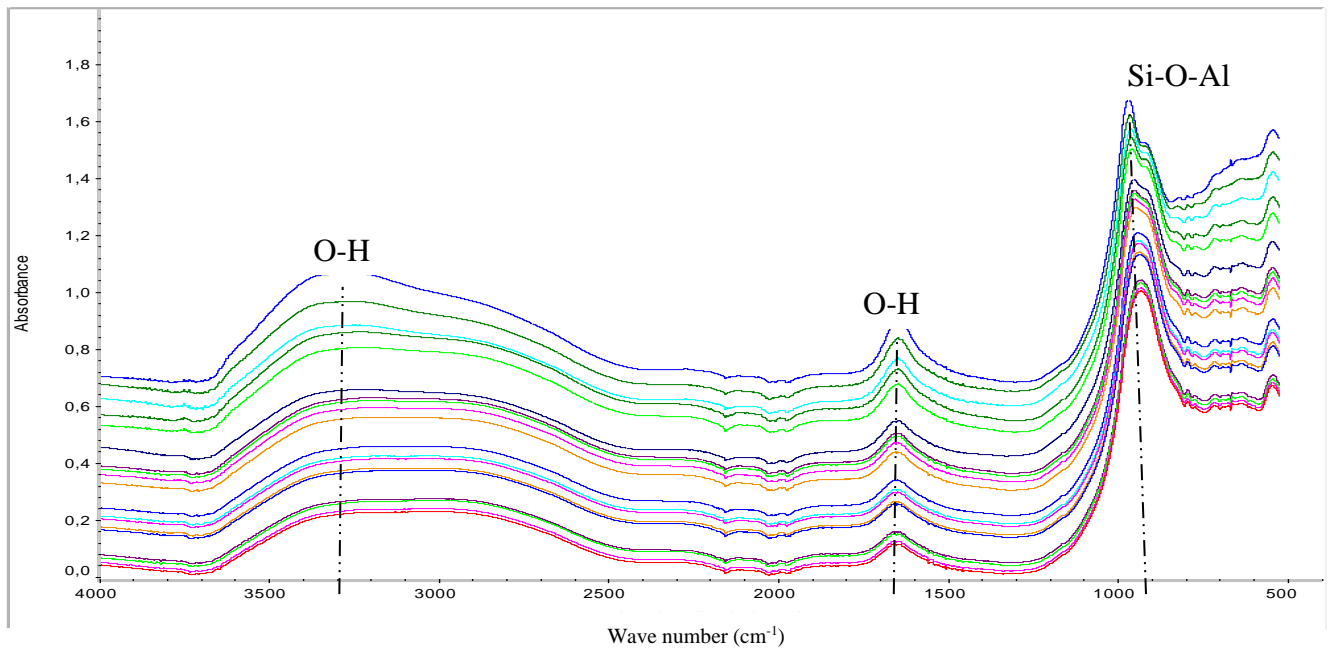


**Figure 13:** The follow-up of the evolution of the reaction of geopolymerization by FTIR

The follow-up of the evolution of the reaction of geopolymerization was studied by estimating the shift of the bonds Si-O-Al which is substituted from Si-O-Si bonds. The shift values were plotted against different samples (Figure 14). The figure showed the variation of shift value for C5, C6, C14, C15, C19 and C20 which were respectively 7.26, 6.55, 36.2, 13.49, 38.7 and 34.65  $\text{cm}^{-1}$ . The total displacement of the band is varied, where the lowest value was 6.55  $\text{cm}^{-1}$  for C6. This low value it can be related to a final structure composed from various networks (geopolymer matrix and aluminosilicate gel) due to the abundance of carbonate in all compositions with A4 also to the heterogeneity of the clays [4]. The increasing shift from 6.55 to 13.49  $\text{cm}^{-1}$  by increasing the quantity of A1c added, resulted from the enrichment of the compounds by kaolinite. The highest value of shift was of 38.7  $\text{cm}^{-1}$  for C19. This last value is near from the value announced for geopolymer materials of 40  $\text{cm}^{-1}$ [39]. This result can be explained by the presence of a higher amount of metakaolin comes from the calcined clay and the pure metakaolin which are more reactive in alkaline solution and this value is near of the one of composition C14 (36.2  $\text{cm}^{-1}$ ) based on calcined clay A1c alone.

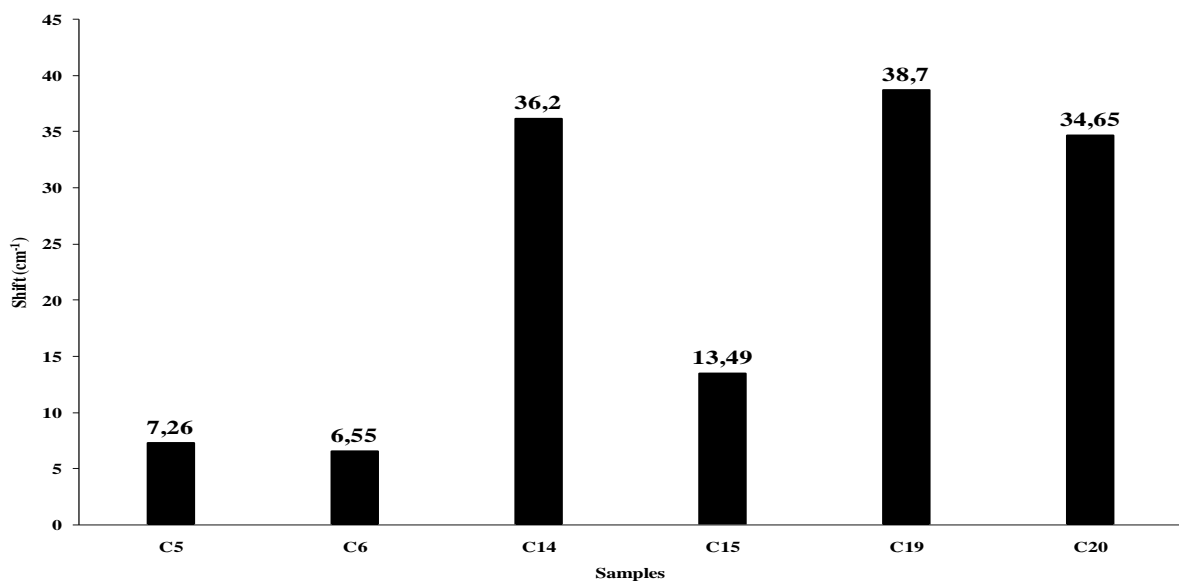


**Figure 14:** Si-O-Si to Si-O-Al shift during polycondensation reaction obtained from FTIR investigations.

From the molar percentages of Si, Al and K, the different compositions have been studied in ternary phase diagram (Figure 15). The diagram contains four zones where each sample was plotted.

The figure showed that some of elaborated materials belong to sedimented material (zone III) and other was between zone I and III, they were more or less near to the geopolymer zone. These results are consistent with the data previously discussed in the study of the displacement of the Si-O-M band.

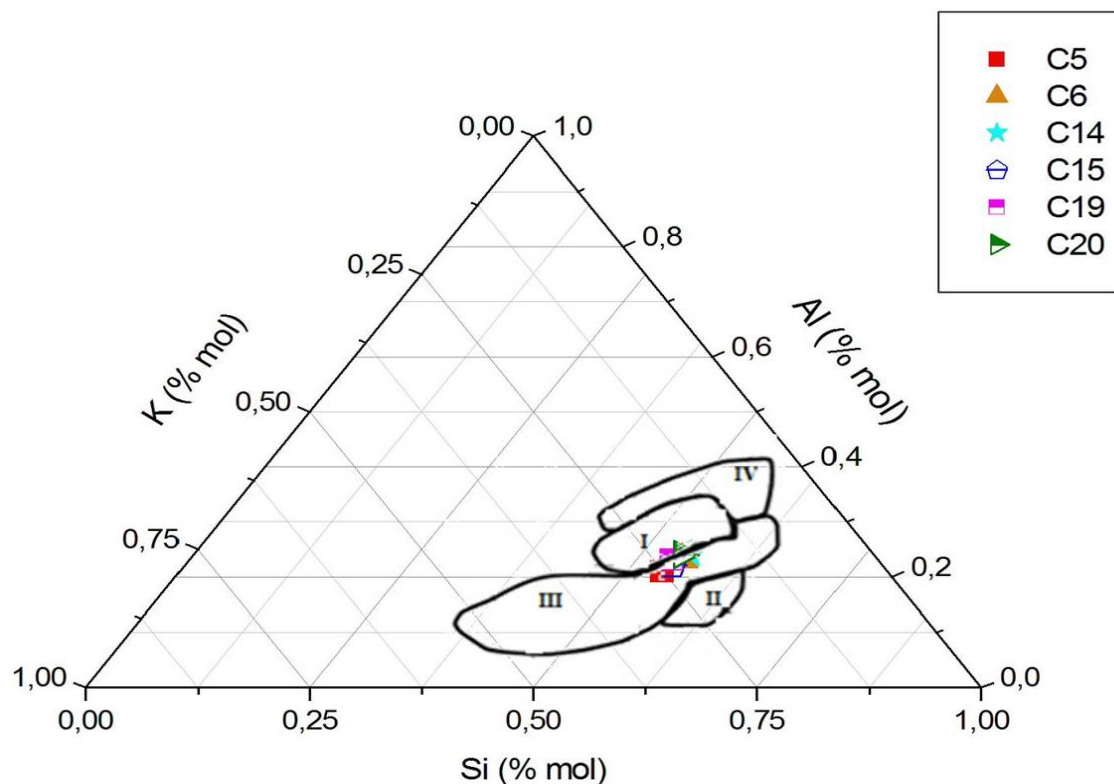


**Figure 15:** Existence domains of synthesized materials on Si–Al–K ternary (I geopolymer, II gel, III sedimented material and IV hardening material)

## Conclusion

The mineralogical and chemical characterization of the two Moroccan clays A1 and A4 revealed that these raw materials contain different clay fraction presented as a mixture of clay phases (Illite, Chlorite, Muscovite, Kaolinite ...). Various quantities of kaolinite were found, where A1 had a kaolin content of 40.82 % accompanied by other minerals. Due to their chemical composition, those materials have different reactivity.

To understand the effect of the mineralogical and chemical composition of those Moroccan clay on the elaboration of geopolymer, many samples were prepared and the investigation of the formation of geopolymer or other networks were performed by FTIR, thus the shift of the band attributed to the Si-O-M bond.

These data proved that, on one hand the reactive and the kaolin rich clay A1 is able to provide homogenous consolidated materials after calcination which was obtained by that Moroccan clay alone in an alkaline solution. On the other hand the presence of carbonate especially calcium carbonate on clay limits the formation not only of geopolymers but also of consolidated materials. Therefore a solution may be to introduce metakaolin in the formulation of geopolymers using these Moroccan clays or to use them as fillers for the elaboration of those materials.

The synthesized materials provide good potential for Moroccan clays in the synthesis of geopolymers. After their synthesis they will need to be characterized. Such a promising aspect requires further investigation.

## References

1. Vieira C.M.F., Sanchez R., Monteiro S.N., *Constr. Build. Mater.*, 22 (2008) 781.
2. Gualtieri M.L., Gualtieri A.F., Gagliardi S., Ruffini P., Ferrari R., Hanuskova M., *Appl. Clay Sci.*, 49 (2010) 269.
3. Murray H.H., Occurrences, Processing and Application of Kaolins, Bentonites, Palygorskite–Sepiolite, and Common Clays, first ed. *Elsevier*, Oxford (2007).
4. Selmani S., Essaidi N., Gouny F., Bouaziz S., Joussein E., Driss A., Sdiri A., Rossignol S., *J. of African Earth Sci.* 103 (2015) 113.
5. Mbey J.A., Hoppe S., Thomas F., *Carbohydr. Polym.*, 88 (2012) 213.
6. Mbey J.A., Thomas F., NgallySabouang C.J., Liboum F., Njopwouo D., *Appl. Clay Sci.*, 83 (2013) 327.
7. TchakouteKouamo H., Elimbi A., Mbey J.A., NgallySabouang C.J., Njop-wouo D., *Constr. Build. Mater.*, 35 (2012) 960.
8. TchakouteKouamo H., Mbey J.A., Elimbi A., KenneDiffo B.B., NjopwouoD., *Ceram. Int.*, 39 (2013) 1613.
9. Davidovits J., *Geopolymer Chemistry and Applications*. Second Ed. Saint-Quentin, France: Geopolymer Institute; (2008).
10. Zhang Y.J., Li S., Wang Y.C., Xu D.L., *J Non-Cryst Solids*, 358 (2012) 620.
11. Verdolotti L., Iannace S., Lavorgna M., Lamanna R., *J Mater Sci*, 43 (2008) 865.
12. Ferone C., Liguori B., Capasso I., Colangelo F., Cioffi R., Cappelletto E., Di Maggio R., *Appl. Clay Sci.* 107 (2015) 195.
13. Tchakoute Kouamo H., Elimbi A., Mbey J.A., Ngally Sabouang C.J., Njop-wouo D., *Constr. Build. Mater.*, 35 (2012) 960.
14. Elfil H., Srasra E., Dogguy M., *J. Thermal Anal.*, 44 (1995) 663.
15. Odilon Kikouamane J.R., *Appl. Clay Sci.* 43 (2009) 135.
16. Marianne LE TROEDEC, Caractérisation des interactions physico-chimiques dans un matériau composite à base de phyllosilicates, de chaux et de fibres cellulose, Le 1er décembre 2009, UNIVERSITE DE LIMOGES, Emna Errais et al (2011).
17. Ravisanka J., Mineralogical, *J. of Chemistry* 7 (2010) 185.
18. Marinez J. R., *J. of Chemical Physics* 109 (1998) 7511.
19. Criado M., Polomo A., A. Fernandez, Jimenez, *Fuel* 87 (2005) 2048.
20. Phair J.W., Van Deventer J.S.J., *Int. J. Min. Process* 66 (2002) 1.
21. Aaron R.S., Anderson E., Schauer C., Barsoum M.W., *Constr. Build. Mater.* 23 (2009) 1.
22. Srasra E., Bergaya F., Fripiat J.J., *Clays and Clay Miner.* 42 (1994) 237.
23. Robert M., *Le sol : interface dans l'environnement, ressource pour le développement*. Masson, Paris, (1996).
24. Caglar B., *J. Mol. Struct.* 1020 (2012) 48.
25. Allali F., Monsif M., Idrissi Kandri N., Zerouale A., *J. Mater. Environ. Sci.* 5 (2014) 2205.
26. koumtoudji N., lecomte G., transformations thermiques, organisation structurale et frittage des composés kaolinite-muscovite, 08 décembre (2004).
27. Shvarzman A., Kovler K., Grader G.S., Shter G.E., *Cement and Concrete Research* 33 (2003) 405.
28. Ress C.A., Provis J.L., Luckey G.C., Van Deventer J.S.J., *Langmuir* 23 (2007) 8170.
29. Essaidi N., Samet B., Baklouti S., Rossignol S., *Appl. Clay Sci.* 88–89 (2014) 221.
30. Elimbi A., Tchakoute H.K., Njopwouo D., *Constr. Build. Mater.* 25 (2011) 2805.
31. Mackenzie K. J. D., Smith M. E., *Multinuclear Solid-State NMR of Inorganic Materials*; Pergamon Press: Oxford, U.K., (2002).
32. Elaiopoulos K., *Microp. Mesop. Mat.*, 134 (2010) 29.
33. Franco F., Cecila J.A., Perez-Maqueda L.A., Perez-Rodriguez J.L., Gomes C.S.F., *Appl. Clay Sci.* 35 (2007) 119.
34. Madéjova J., *Vib. Spectrosc.* 31 (2003) 1.
35. Hajji L., *Spectrochimica Acta Part A: Molecular and Biomolecular Spectroscopy*, (2014).
36. Matusik J., Kłapyta Z., Olejniczak Z., *Appl. Clay Sci.* 83 (2013) 426.
37. Ptacek P.; Opravil T.; Soukal F., *Solid State Sci.* 26 (2013) 53.

38. Mantovani M., Escudero A., Becerro A.I., *Clays and Clay Minerals* 57 (2009) 302.
39. Prud'homme E., Autef A., Essaidi N., Michaud P., Samet B., Joussein E., Rossignol S., *Appl. Clay Sci.* 73 (2013) 26.

(2017); <http://www.jmaterenvironsci.com>